

# Deeply Virtual Compton Scattering and Meson Production at JLab/CLAS

Hyon-Suk Jo

Institut de Physique Nucléaire d'Orsay, 91406 Orsay, France

## Abstract

This report reviews the recent experimental results from the CLAS collaboration (Hall B of Jefferson Lab, or JLab) on Deeply Virtual Compton Scattering (DVCS) and Deeply Virtual Meson Production (DVMP) and discusses their interpretation in the framework of Generalized Parton Distributions (GPDs). The impact of the experimental data on the applicability of the GPD mechanism to these exclusive reactions is discussed. Initial results obtained from JLab 6 GeV data indicate that DVCS might already be interpretable in this framework while GPD models fail to describe the exclusive meson production (DVMP) data with the GPD parameterizations presently used. An exception is the  $\phi$  meson production for which the GPD mechanism appears to apply. The recent global analyses aiming to extract GPDs from fitting DVCS CLAS and world data are discussed. The GPD experimental program at CLAS12, planned with the upcoming 12 GeV upgrade of JLab, is briefly presented.

## Introduction

Generalized Parton Distributions take the description of the complex internal structure of the nucleon to a new level by providing access to, among other things, the correlations between the (transverse) position and (longitudinal) momentum distributions of the partons in the nucleon. They also give access to the orbital momentum contribution of partons to the spin of the nucleon.

GPDs can be accessed via Deeply Virtual Compton Scattering and exclusive meson electroproduction, processes where an electron interacts with a parton from the nucleon by the exchange of a virtual photon and that parton radiates a real photon (in the case of DVCS) or hadronizes into a meson (in the case of DVMP). The amplitude of the studied process can be factorized into a hard-scattering part, exactly calculable in pQCD or QED, and a non-perturbative part, representing the soft structure of the nucleon, parametrized by the GPDs. At leading twist and leading order approximation, there are four independent quark helicity conserving GPDs for the nucleon:  $H$ ,  $E$ ,  $\tilde{H}$  and  $\tilde{E}$ . These GPDs are functions depending on three variables  $x$ ,  $\xi$  and  $t$ , among which only  $\xi$  and  $t$  are experimentally accessible. The quantities  $x + \xi$  and  $x - \xi$  represent respectively the longitudinal momentum fractions carried by the initial and final parton. The variable  $\xi$  is linked to the Bjorken variable  $x_B$  through the asymptotic formula:  $\xi = \frac{x_B}{2-x_B}$ . The variable  $t$  is the squared momentum transfer between the initial and final nucleon. Since the variable  $x$  is not experimentally accessible, only Compton Form Factors, or CFFs ( $\mathcal{H}$ ,  $\mathcal{E}$ ,  $\tilde{\mathcal{H}}$  and  $\tilde{\mathcal{E}}$ ), which real parts are weighted integrals of GPDs over  $x$  and imaginary parts are combinations of GPDs at the lines  $x = \pm\xi$ , can be extracted.

The reader is referred to Refs. [1–11] for detailed reviews on the GPDs and the theoretical formalism.

## Deeply Virtual Compton Scattering

Among the exclusive reactions allowing access to GPDs, Deeply Virtual Compton Scattering (DVCS), which corresponds to the electroproduction of a real photon off a nucleon  $eN \rightarrow eN\gamma$ , is the key reaction since it offers the simplest, most straightforward theoretical interpretation in terms of GPDs. The DVCS amplitude interferes with the amplitude of the Bethe-Heitler (BH) process which leads to the exact same final state. In

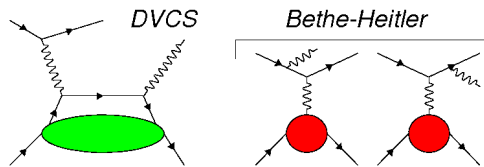


Figure 1: Handbag diagram for DVCS (left) and diagrams for Bethe-Heitler (right), the two processes contributing to the amplitude of the  $eN \rightarrow eN\gamma$  reaction.

the BH process, the real photon is emitted by either the incoming or the scattered electron while in the case of DVCS, it is emitted by the target nucleon (see Figure 1). Although these two processes are experimentally indistinguishable, the BH is well known and exactly calculable in QED. At current JLab energies (6 GeV), the BH process is highly dominant (in most of the phase space) but the DVCS process can be accessed via the interference term rising from the two processes. With a polarized beam or/and a polarized target, different types of asymmetries can be extracted: beam-spin asymmetries ( $A_{LU}$ ), longitudinally polarized target-spin asymmetries ( $A_{UL}$ ), transversely polarized target-spin asymmetries ( $A_{UT}$ ), double-spin asymmetries ( $A_{LL}$ ,  $A_{LT}$ ). Each type of asymmetry gives access to a different combination of Compton Form Factors.

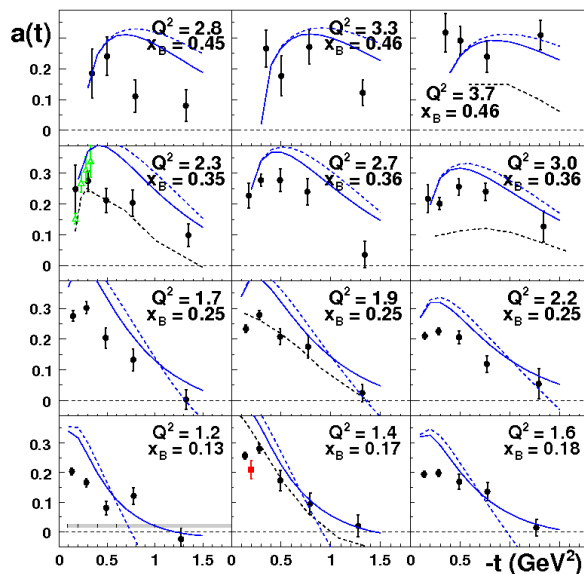


Figure 2: DVCS beam-spin asymmetries as a function of  $-t$ , for different values of  $Q^2$  and  $x_B$ . The (black) circles represent the latest CLAS results [16], the (red) squares and the (green) triangles are the results, respectively, from Ref. [12] and Ref. [20]. The black dashed curves represent Regge calculations [17]. The blue curves correspond to the GPD calculations of Ref. [9] (VGG) at twist-2 (solid) and twist-3 (dashed) levels, with the contribution of the GPD  $H$  only.

The first results on DVCS beam-spin asymmetries published by the CLAS collaboration were extracted using data from non-dedicated experiments [12, 13]. Also using non-dedicated data, CLAS published DVCS longitudinally polarized target-spin asymmetries in 2006 [14]. In 2005, the first part of the e1-DVCS experiment was carried out in the Hall B of JLab using the CLAS spectrometer [15] and an additional electromagnetic calorimeter, made of 424 lead-tungstate scintillating crystals read out via avalanche photodiodes, specially designed and built for the experiment. This additional calorimeter was located at the forward

angles, where the DVCS/BH photons are mostly emitted, as the standard CLAS configuration does not allow detection at those forward angles. This first CLAS experiment dedicated to DVCS measurements, with this upgraded setup allowing a fully exclusive measurement, ran using a 5.766 GeV polarized electron beam and a liquid-hydrogen target. From this experiment data, CLAS published in 2008 the largest set of DVCS beam-spin asymmetries ever extracted in the valence quark region [16]. Figure 2 shows the corresponding results as a function of  $-t$  for different bins in  $(Q^2, x_B)$ . The predictions using the GPD model from VGG (Vanderhaeghen, Guichon, Guidal) [9, 10] overestimate the asymmetries at low  $|-t|$ , especially for small values of  $Q^2$  which can be expected since the GPD mechanism is supposed to be valid at high  $Q^2$ . Regge calculations [17] are in fair agreement with the results at low  $Q^2$  but fail to describe them at high  $Q^2$  as expected. We are currently working on extracting DVCS unpolarized and polarized absolute cross sections from the e1-DVCS data [18].

Having both the beam-spin asymmetries and the longitudinally polarized target-spin asymmetries, a largely model-independent GPD analysis in leading twist was performed, fitting simultaneously the values for  $A_{LU}$  and  $A_{UL}$  obtained with CLAS at three values of  $t$  and fixed  $x_B$ , to extract numerical constraints on the imaginary parts of the Compton Form Factors (CFFs)  $\mathcal{H}$  and  $\bar{\mathcal{H}}$ , with average uncertainties of the order of 30% [19]. Before that, the same analysis was performed fitting the DVCS unpolarized and polarized cross sections published by the JLab Hall A collaboration [20] to extract numerical constraints on the real and imaginary parts of the CFF  $\mathcal{H}$  [21]. Another GPD analysis in leading twist, assuming the dominance of the GPD  $H$  (the contributions of  $\bar{H}$ ,  $E$  and  $\bar{E}$  being neglected) and using the CLAS  $A_{LU}$  data as well as the DVCS JLab Hall A data, was performed to extract constraints on the real and imaginary parts of the CFF  $\mathcal{H}$  [22]. Similar analyses were performed using results published by the HERMES collaboration [23, 24]. A third approach was developed, using a model-based global fit on the available world data to calculate the real and imaginary parts of the CFF  $\mathcal{H}$  [25]. When we compare the different results of those analyses for the imaginary part of  $\mathcal{H}$ , they appear to be relatively compatible (such a comparison plot can be found in Ref. [26]).

## Deeply Virtual Meson Production

The CLAS collaboration published several results on pseudoscalar meson electroproduction ( $\pi^0, \pi^+$ ) [27, 28]. However, those are not reviewed in this paper, limiting itself to vector mesons.

CLAS published cross-section measurements for the following vector mesons:  $\rho^0$  [29, 30],  $\omega$  [31] and  $\phi$  [32, 33], contributing significantly to the world data on vector mesons with measurements in the valence quark region, corresponding to low  $W$  ( $W < 5$  GeV). First measurements of  $\rho^+$  electroproduction are being extracted from the e1-DVCS data mentioned above [34].

As the leading-twist handbag diagram is only valid for the longitudinal part of the cross section of those vector mesons, it is required to separate the longitudinal and transverse parts of the cross sections extracted from the experimental data by analyzing the decay angular distribution of the meson. Figure 3 shows the longitudinal cross sections of the  $\rho^0$  meson production  $\sigma_L(\gamma^*p \rightarrow p\rho^0)$  as a function of  $W$  at fixed  $Q^2$ , for different bins in  $Q^2$ . As a function of increasing  $W$ , those cross sections first drops at low  $W$  ( $W < 5$  GeV, corresponding to the valence quark region) and then slightly rise at higher  $W$ . The longitudinal cross sections of the  $\omega$  meson production seems to show the same behavior as a function of  $W$  as the one observed for the  $\rho^0$  meson. The GPD-based predictions from VGG and from GK (Goloskokov, Kroll) [35] describe quite well those results at high  $W$  but both GPD models fail by large to reproduce the behavior at low  $W$  (see the curves on Figure 3). The  $\phi$  meson production, which is mostly sensitive to gluon GPDs, is a different case as its longitudinal cross sections as a function of  $W$  show a different behavior by continuously rising with increasing  $W$  all the way from the lowest  $W$  region; these cross sections are very well described by the GPD model predictions [36]. The reason why the GPD models fail to describe the data for the  $\rho^0$  and  $\omega$  mesons at low  $W$  (valence quark region) is unsure at this point. The handbag mechanism might not be dominant in the low  $W$  valence region as the minimum value of  $|-t|$  increases with decreasing  $W$  and higher-twist effects grow with  $t$ . Another possibility is that the handbag mechanism might actually be dominant in the low  $W$  valence region but there is an important contribution missing in the GPD models.

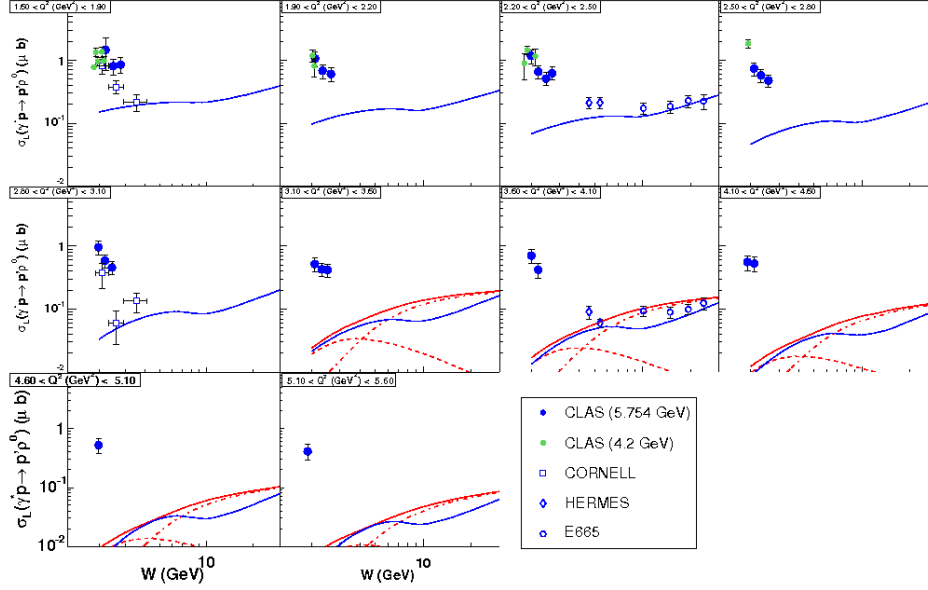


Figure 3: Longitudinal cross sections for  $\rho^0$  as a function of  $W$  at fixed  $Q^2$  (CLAS and world data). The results from CLAS are shown as full circles. The blue curves are VGG GPD-based predictions. The red curves represent GK GPD-based predictions: total (solid), valence quarks (dashed), sea quarks and gluons (dot-dashed).

## DVCS and DVMP at CLAS12

With the upcoming 12 GeV upgrade of JLab's CEBAF accelerator, the instrumentation in the experimental halls will be upgraded as well. In Hall B, the CLAS detector will be replaced by the new CLAS12 spectrometer, under construction, with the study of Generalized Parton Distributions as one of the highest priorities of its future experimental program. The experiments currently proposed have the following goals:

- DVCS beam-spin asymmetries on the proton,
- DVCS longitudinal target-spin asymmetries on the proton,
- DVCS transverse target-spin asymmetries on the proton,
- DVCS on the neutron,
- DVCS unpolarized and polarized cross sections,
- DVMP: pseudoscalar meson electroproduction,
- DVMP: vector meson electroproduction.

To study DVCS on the neutron, a central neutron detector was designed to be added to the base equipment of the CLAS12 spectrometer. A combined analysis of DVCS on the proton and on the neutron allows flavor separation of GPDs.

JLab 12 GeV will provide high luminosity ( $L \sim 10^{35} \text{cm}^{-2} \text{s}^{-1}$ ) for high accuracy measurements to study GPDs in the valence quark region and test the models on a large  $x_B$  scale. The new CLAS12 spectrometer, with its large acceptance allowing measurements on a large kinematic range, will be perfectly fitted for a rich GPD experimental program.

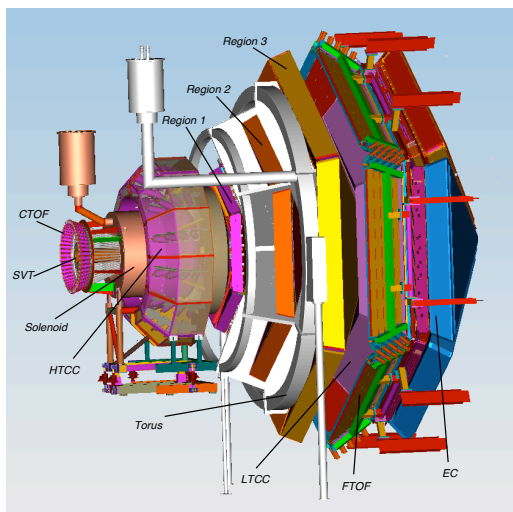


Figure 4: The CLAS12 detector currently under construction.

## Conclusions

The CLAS collaboration produced the largest set of data for DVCS and exclusive vector meson production ever extracted in the valence quark region. The VGG GPD model fairly agrees with the DVCS asymmetry data at high  $Q^2$  but fails to reproduce it at lower  $Q^2$ . As for the exclusive vector meson data, GPD models describe well the longitudinal cross sections at high  $W$  (region corresponding to sea quarks and/or gluons) which seem to be interpretable in terms of leading-twist handbag diagram (quark/gluon GPDs) but fail by large for  $W < 5$  GeV (corresponding to the valence quark region) except for the  $\phi$  meson for which the GPD formalism seems to apply. We need experimental data of higher  $Q^2$  while staying in the valence quark region to extend the DVCS data on a larger kinematic domain and provide more constraints for the GPD models, and to test the GPD mechanism validity regime for DVMP. JLab 12 GeV will provide high luminosity for high accuracy measurements to test models on a large  $x_B$  scale and thus will be a great facility to study GPDs in the valence quark region. The new CLAS12 spectrometer, with its large acceptance, will be well suited for a rich and exciting GPD experimental program.

## Acknowledgments

Thanks to P. Stoler and R. Ent for the opportunity to give this presentation. Thanks to M. Guidal and S. Niccolai for useful discussions and for providing slides used for the preparation of this talk.

## References

- [1] D. Müller, D. Robaschik, B. Geyer, F.-M. Dittes, and J. Horejsi, *Fortschr. Phys.* **42**, 101 (1994).
- [2] X. Ji, *Phys. Rev. Lett.* **78**, 610 (1997); *Phys. Rev. D* **55**, 7114 (1997).
- [3] A.V. Radyushkin, *Phys. Lett. B* **380** (1996) 417; *Phys. Rev. D* **56**, 5524 (1997).
- [4] J.C. Collins, L. Frankfurt and M. Strikman, *Phys. Rev. D* **56**, 2982 (1997).
- [5] K. Goeke, M.V. Polyakov and M. Vanderhaeghen, *Prog. Part. Nucl. Phys.* **47**, 401 (2001).
- [6] M. Diehl, *Phys. Rept.* **388**, 41 (2003).
- [7] A.V. Belitsky, A.V. Radyushkin, *Phys. Rept.* **418**, 1 (2005).

- [8] M. Guidal, *Prog. Part. Nucl. Phys.* **61**, 89 (2008).
- [9] M. Vanderhaeghen, P.A.M. Guichon, and M. Guidal, *Phys. Rev. D* **60**, 094017 (1999).
- [10] M. Guidal, M.V. Polyakov, A.V. Radyushkin and M. Vanderhaeghen, *Phys. Rev. D* **72**, 054013 (2005).
- [11] A. Belitsky, D. Müller and A. Kirchner, *Nucl. Phys. B* **629**, 323 (2002).
- [12] S. Stepanyan *et al.* (CLAS Collaboration), *Phys. Rev. Lett.* **87**, 182002 (2001).
- [13] G. Gavalian *et al.* (CLAS Collaboration), *Phys. Rev. C* **80**, 035206 (2009).
- [14] S. Chen *et al.* (CLAS Collaboration), *Phys. Rev. Lett.* **97**, 072002 (2006).
- [15] B. Mecking *et al.*, *Nucl. Instrum. Meth. A* **503**, 513 (2003).
- [16] F.X. Girod *et al.* (CLAS Collaboration), *Phys. Rev. Lett.* **100**, 162002 (2008).
- [17] J.M. Laget, *Phys. Rev. C* **76**, 052201(R) (2007).
- [18] H.S. Jo, Ph.D. thesis, Université Paris-Sud, Orsay, France (2007).
- [19] M. Guidal, *Phys. Lett. B* **689**, 156 (2010).
- [20] C. Munoz Camacho *et al.* (JLab Hall A Collaboration), *Phys. Rev. Lett.* **97**, 262002 (2006).
- [21] M. Guidal, *Eur. Phys. J. A* **37**, 319 (2008) [Erratum-*ibid.* **A 40**, 119 (2009)].
- [22] H. Moutarde, *Phys. Rev. D* **79**, 094021 (2009).
- [23] M. Guidal and H. Moutarde, *Eur. Phys. J. A* **42**, 71 (2009).
- [24] M. Guidal, *Phys. Lett. B* **693**, 17 (2010).
- [25] K. Kumerički and D. Müller, *Nucl. Phys. B* **841**, 1 (2010).
- [26] K. Kumerički and D. Müller, arXiv:1008.2762 [hep-ph].
- [27] R. De Masi *et al.* (CLAS Collaboration), *Phys. Rev. C* **77**, 042201(R) (2008).
- [28] K. Park *et al.* (CLAS Collaboration), *Phys. Rev. C* **77**, 015208 (2008).
- [29] C. Hadjidakis *et al.* (CLAS Collaboration), *Phys. Lett. B* **605**, 256-264 (2005).
- [30] S. Morrow *et al.* (CLAS Collaboration), *Eur. Phys. J. A* **39**, 5-31 (2009).
- [31] L. Morand *et al.* (CLAS Collaboration), *Eur. Phys. J. A* **24**, 445-458 (2005).
- [32] K. Lukashin *et al.* (CLAS Collaboration), *Phys. Rev. C* **63**, 065205 (2001).
- [33] J. Santoro *et al.* (CLAS Collaboration), *Phys. Rev. C* **78**, 025210 (2008).
- [34] A. Fradi, Ph.D. thesis, Université Paris-Sud, Orsay, France (2009).
- [35] S.V. Goloskokov and P. Kroll, *Eur. Phys. J. C* **42**, 281 (2005); *Eur. Phys. J. C* **50**, 829 (2007).
- [36] S.V. Goloskokov, arXiv:0910.4308 [hep-ph].